Crosstalk Performance of Integrated Optical Cross-Connects

Chretien G. P. Herben, Xaveer J. M. Leijtens, Peter Maat, Hans Blok, *Member, IEEE,* and Meint K. Smit, *Associate Member, IEEE*

***Abstract*—Crosstalk performance of monolithically integrated multiwavelength optical cross-connects (OXC's) depends strongly on their architecture. In this paper, a semiquantitative analysis of crosstalk in 11 different architectures is presented. Two architectures are analyzed numerically in more detail and the results of the analysis show good agreement with previously reported experimental results.**

***Index Terms*—Integrated optics, optical cross-connect (OXC), semiconductor waveguides, wavelength division multiplexing (WDM).**

I. Introduction

OPTICAL cross-connects (OXC's) are key components in advanced wavelength division multiplexed (WDM) networks [1]. At present, OXC's used in network experiments consist of large numbers of discrete components, which makes them costly and voluminous. To reduce both cost and dimensions, integration will be necessary. Several integrated OXC's and add–drop multiplexers have been reported [2]–[8]. First integrated wavelength selective switches were realized in silica technology using thermooptic switches [2], [4], [6]. On InP, the first devices reported [3], [5] operated only at transverse electric (TE)-polarization. Recently, we reported the first integrated polarization independent OXC's on InP [7], [8].

These integrated OXC's consist of phased-array demultiplexers [9] monolithically integrated with electrooptic space switches. The connection between the PHASAR(s) and switches can be done in many ways. First applications used looped-back configurations [10]. These configurations, however, result in power penalties caused by signal-crosstalk beat noise. Improved designs using fold-back optical paths were proposed to avoid the crosstalk penalties [11]–[13].

Zhou *et al.* [14] reported a crosstalk comparison between three multiwavelength cross-connect architectures. The configurations compared used different switch architectures. They found that crosstalk improvement could be realized by introducing a wavelength selective filter between the switch output and the multiplexer input.

In monolithic integration, combination of wavelength filters with multiplexers is considered difficult. In this article, we focus on different connection-schemes between demultiplexers, switches and multiplexers. The OXC architectures that will be discussed are all are N-wavelength 2×2 OXC's based on integration of demultiplexers with 2×2 space switches. We restrict ourselves to 2×2 OXC's, these are the most elementary OXC's and can be used in interconnecting links and rings and as building blocks in larger cross-connects. Further, we restrict ourselves to architectures with single wavelength operation for the switches because of the limited bandwidth of semiconductor-based integrated switches.

In this article, we present a semiquantitative analysis of the crosstalk performance of eleven different architectures for 2×2 cross-connects (Section II). Crosstalk is investigated by analyzing the number of possible crosstalk paths, and estimating the performance from the total number of dominant terms (= paths) contributing to the crosstalk. For two of these architectures a detailed numerical analysis is presented (Section III): one for the first architecture which we realized experimentally and a second one for the structure which we consider optimal based on the semiquantitative analysis, this structure has been realized and reported recently [8]. For these two devices experimental and simulation results are compared and found to be in good agreement (Section IV).

II. Semiqualitative Analysis of Different Cross-Connect Configurations

Three basic operations that have to be performed in an integrated optical cross-connect are demultiplexing, space switching and multiplexing. To ensure optimal performance of the total device the spectral responses of the demultiplexer and multiplexer have to be aligned sufficiently accurate. In a 2×2 OXC, in general, two demultiplexing and two multiplexing operations have to be performed. Misalignment of the spectral responses of the PHASAR's used for the (de)multiplexing operations results in increased losses. Nonuniformity of the layers and composition of the wafer make it hard to perfectly match the spectral responses of multiple PHASAR's on a single chip. When no active tuning of the separate demultiplexers is used, it is advantageous to combine multiple (de)multiplex operations within a single PHASAR router. A perfect match of the wavelength response is obtained at the price of larger phased array.

Manuscript received July 17, 1998; revised March 22, 1999. This work was supported in part by the ACTS projects AC-065 BLISS and AC-332 APEX.

C. G. P. Herben, X. J. M. Leijtens, and M. K. Smit are with the Faculty of Information Technology and Systems, Photonic Integrated Circuits Group, Delft University of Technology, Delft NL-2600 GA The Netherlands.

P. Maat is with the Faculty of Applied Sciences, Research Group for Optics, Delft University of Technology, Delft NL-2600 GA The Netherlands.

H. Blok is with the Faculty of Information Technology and Systems, Laboratory of Electromagnetic Research, Delft University of Technology, Delft NL-2600 GA The Netherlands.

Publisher Item Identifier S 0733-8724(99)05525-5.

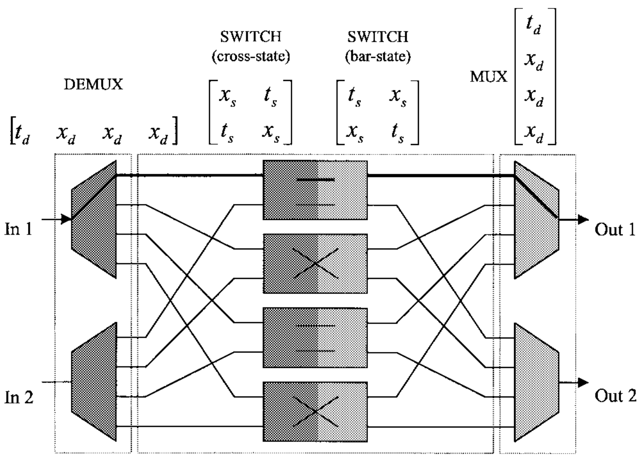

Fig. 1. Transmission matrices of the subcomponents that form the OXC.

We looked at various ways of constructing an N-wavelength 2 × 2 integrated optical cross-connect. Eleven different configurations have been distinguished, using a single up to four separate phased-arrays. All architectures use N 2 × 2 space switches. For each configuration the transmission coefficients of possible light paths have been determined. In order to describe the number of crosstalk contributions we use the following notation: t stands for transmission, which means that the signal follows the designed path, and x for crosstalk, which means that the signal takes routes it was not supposed to take.

In Fig. 1, the most straightforward scheme of a 2 × 2 OXC is depicted and the transmission matrices of all components are indicated. For our analysis, we are only interested in the approximate signal levels; all transmission coefficients are denoted as t, all crosstalk coefficients are denoted as x. The suffixes d, s, m, and c refer to demultiplexer, switch, multiplexer and combiner, respectively. The transfer matrix of the whole OXC for one switching state (bar state) for wavelength 1 can be written as

$$\begin{bmatrix}\mathrm{Out}_1\\ \mathrm{Out}_2\end{bmatrix} = \begin{bmatrix} t_d & x_d & x_d & x_d & 0 & 0 & 0 & 0\\ 0 & 0 & 0 & 0 & t_d & x_d & x_d & x_d\end{bmatrix} \cdot \begin{bmatrix} t_s & 0 & 0 & 0 & x_s & 0 & 0 & 0\\ 0 & x_s & 0 & 0 & 0 & t_s & 0 & 0\\ 0 & 0 & t_s & 0 & 0 & 0 & x_s & 0\\ 0 & 0 & 0 & x_s & 0 & 0 & 0 & t_s\\ x_s & 0 & 0 & 0 & t_s & 0 & 0 & 0\\ 0 & t_s & 0 & 0 & 0 & x_s & 0 & 0\\ 0 & 0 & x_s & 0 & 0 & 0 & t_s & 0\\ 0 & 0 & 0 & t_s & 0 & 0 & 0 & x_s\end{bmatrix} \cdot \begin{bmatrix} t_m & 0\\ x_m & 0\\ x_m & 0\\ x_m & 0\\ 0 & t_m\\ 0 & x_m\\ 0 & x_m\\ 0 & x_m\end{bmatrix} \cdot \begin{bmatrix}\mathrm{In}_1\\ \mathrm{In}_2\end{bmatrix}$$

or

$$\begin{bmatrix}\mathrm{Out}_1\\ \mathrm{Out}_2\end{bmatrix} = \begin{bmatrix} t_d t_s t_m + x_d t_s x_m + 2x_d x_s x_m & t_d t_s t_m + 2x_d t_s x_m + x_d x_s x_m\\ t_d x_s t_m + 2x_d t_s x_m + x_d x_s x_m & t_d t_s t_m + x_d t_s x_m + 2x_d x_s x_m\end{bmatrix} \cdot \begin{bmatrix}\mathrm{In}_1\\ \mathrm{In}_2\end{bmatrix}.$$

In the cross elements of the matrix, which should ideally be zero, we see three types of elements, one containing one factor x, one containing two factors x and one containing three factors x. Usually the x-factors will be much smaller than the t-factors (in dB's: a few dB's for t, 20–40 dB for x), so the terms with the smallest number of x-factors will be the dominant crosstalk terms. If several crosstalk terms with comparable magnitude are present then they may interfere constructively or destructively, on average the total crosstalk will increase with an increasing number of terms, so the total number of dominant crosstalk terms is a measure for the performance. In the following, we will compare eleven different cross-connect configurations as depicted in Fig. 2 by considering the total number of dominant crosstalk terms. We restrict ourselves at this point to signals originating from one of the inputs and look at both outputs. Since all these contributions originate from the same source and the path-lengths lie within the coherence length of the laser, they will interfere coherently. Interference between signals from different inputs will depend on phase and polarization matching and be predominantly incoherent. These contributions will be briefly discussed at the end of the section. Finally we restrict ourselves to crosstalk at the same wavelength as the signal (intraband crosstalk), since this cannot be filtered out using narrow-band filters.

The 11 different architectures are grouped after the number of operations performed within the PHASAR's. Starting from a single (de)multiplexing operation in the PHASAR(s) (thus using four separate PHASAR's), and ending with all four (de)multiplexing operations performed within a single PHASAR.

A. Configurations with Four PHASARS

Starting with the most straightforward scheme, the first configuration (A) (Figs. 1 and 2) uses four separate 1 × N PHASAR's. First two separate PHASAR's demultiplex the light from both inputs. The signals are then sorted by wavelength and routed to the switches. After the switches the signals are routed to the second pair of PHASAR's that multiplex the light again. The following signal-to-crosstalk contributions can be derived. If we look at input 1 from configuration A, the designed path for the first wavelength has a transmission $t_d t_s t_m$ (thick line). Other possible paths from input 1 to output 1 are dependent on the states of the other switches. If a switch is in the bar-state a path $x_d t_s x_m$ is possible from input 1 to output 1. Otherwise, a path $x_d x_s x_m$ is present from input 1 to output 1. This means that depending on the state of the switches up to $N-1$ contributions $x_d t_s x_m$ can be present in output 1. Since all possible contributions contain at least two crosstalk terms they are of order two, we will denote them as

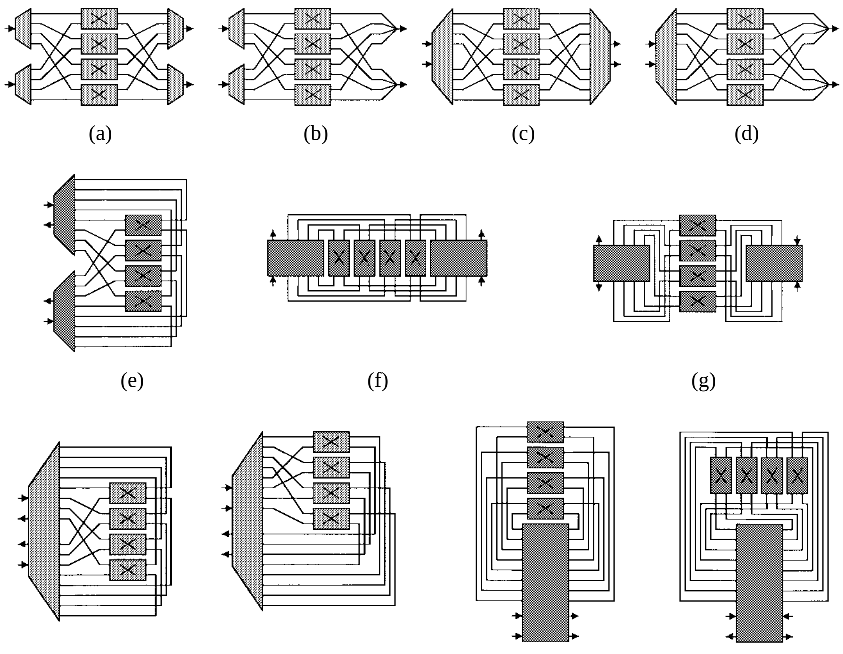

Fig. 2. The 11 OXC configurations used in the semiqualitative analysis.

$O(x^2)$. From input 1 to the undesired output 2 we find in a similar way the contribution $t_d x_s t_m$ and also up to $N-1$ terms of second-order crosstalk (terms with more than one x, i.e., $x_d t_s x_m$). We can thus write the transmission of the device as

$$t_d t_s t_m + O(x^2) \tag{1}$$

for the signal in the desired output. For the unwanted output we find the crosstalk

$$t_d x_s t_m + O(x^2). \tag{2}$$

From (2) it is clear that only the switch contributes to first-order crosstalk.

In the second concept (B) power combiners have replaced the multiplexers. This results in an inherent loss penalty of 6 dB, but reduces the number of phased arrays. In terms of crosstalk performance degradation is expected compared to configuration A since the power-combiners lack the filter function of the multiplexers. All wavelengths from all inputs of the power-combiner can reach all outputs, leading to up to $N-1$ terms $x_d t_s t_c$ in stead of the second-order terms $x_d t_s x_m$ in configuration A. For this configuration we can write for the signal-path

$$t_d t_s t_m + (N-1\,\text{to}\,0) \times x_d t_x t_c + O(x^2). \tag{3}$$

And for the crosstalk, we now get

$$t_d x_s t_m + (0\,\text{to}\,N-1) \times x_d t_s t_c + O(x^2). \tag{4}$$

Compared to configuration A, we can clearly see the increase in the number of crosstalk terms. Not only the switch is contributing to the first-order crosstalk, but also the demultiplexer. The number of crosstalk terms containing the demultiplexer crosstalk depends on the state of the switches.

B. Configurations with Two PHASAR's

A problem in configuration A is the frequency alignment of the multiplexers and demultiplexers. This problem can be reduced by combining both demultiplexers in one 2 $\times$ $2N$ PHASAR, and both multiplexers as well (configuration C). The number of PHASAR's can thus be reduced to two. However, crosstalk from each of the inputs can now easily access paths corresponding to the other input ($t_d t_s x_m$ and $x_d t_s t_m$). We now get the following expression for the crosstalk:

$$t_d t_s x_m + t_d x_s t_m + x_d t_s t_m + O(x^2). \tag{5}$$

The first-order crosstalk now contains not only a switch contribution, but also one from the demultiplexer and one originating from the multiplexer crosstalk. The overall performance is thus expected to be worse than that of configuration A.

As before we can replace the multiplexing PHASAR in configuration C by power-combiners resulting in configuration D. This configuration now contains only one PHASAR and therefore frequency misalignment is impossible. The crosstalk performance is now given by

$$t_d x_s t_m + (N-1) \times x_d t_s t_c + O(x^2). \tag{6}$$

When configurations B (4) and D (6), that are both using power combiners, are compared it is seen that always $(N-1)$ first-order demultiplexer crosstalk terms are present in (6). These terms are caused by the fact that only a single PHASAR is used for demultiplexing the signals of both inputs.

An architecture that uses two 2 $\times$ $2N$ PHASAR's like in concept C, but that has only counterpropagating signals present within each PHASAR is shown in configuration E. The crosstalk paths $t_d t_s x_m$ and $x_d t_s t_m$ are no longer possible in this arrangement. The crosstalk performance of this device is given by

$$t_d x_s t_m + O(x^2). \quad (7)$$

Only one first-order crosstalk term, caused by the switch is present in (7). The performance of this configuration is expected to be better than C, and comparable to that of concept A.

From a layout point of view a loop-back configuration is very attractive because of its simple connection scheme. Configuration F shows a looped-back version using two $(N+1) \times (N+1)$ PHASAR's. A clear disadvantage is the fact that crosstalk from the input can directly access the output (term x_d). The looped-back paths also allow for signals passing twice through the loops while still containing only a single crosstalk term $(t_d t_s x_m t_s t_m)$. Transmission performance of this configuration can be expressed by

$$t_d t_s t_m + x_d + t_d t_s x_m t_s t_m + O(x^2). \quad (8)$$

This time the crosstalk terms are present in the signal port. Both crosstalk terms x_d and $t_d t_s x_m t_s t_m$ can be avoided by making the connections in a fold-back way as is done in configuration G. Crosstalk performance of this concept is expected to be comparable to that of A and E and given by (2 or 7).

C. Configurations with a Single PHASAR

It is also possible to realize an N-wavelength 2 × 2 OXC using only a single PHASAR. The wavelength response of all (de)multiplex filters is now inherently matched. Concept H is derived from E by merging the two PHASAR's into a single 4 × 4N PHASAR. The crosstalk performance is expected to be worse than the configurations A and E because of the copropagating signals within the PHASAR that lead to additional crosstalk paths. We can write the crosstalk performance of configuration H as

$$t_d t_s x_m + t_d x_s t_m + x_d t_s t_m + O(x^2). \quad (9)$$

As before in configuration C terms $t_d t_s x_m$ and $x_d t_s t_m$ containing crosstalk contributions of the (de)multiplexer, are present. Combining the PHASAR's from configuration C into a single PHASAR results in concept I, which is expected to have similar performance as configuration H, since the crosstalk performance is also given by (9). Compared to configuration C the performance does not suffer from the combination of the separate (de)multiplexers into one. This is true at least for the first-order crosstalk terms. The number of second-order terms (terms with more than one x), however, has increased compared to configurations H and I.

A loop-back version using a single PHASAR is shown in configuration J, which follows from concept F by merging the PHASAR's into a single $(3N+1) \times (3N+1)$ PHASAR. Again as in F crosstalk from the inputs can directly access the outputs (term x_d). The "loop-back" crosstalk term that follows from signals passing twice trough the loops $(t_d t_s x_m t_s t_m)$ is also present, as well as the terms $t_d t_s t_m$ and $x_d t_s t_m$. Crosstalk performance of this configuration is given by (10) and predicts a severely degraded performance as compared to the other configurations

$$x_d + t_d t_s x_m + t_d x_s t_m + x_d t_s t_m + t_d t_s x_m t_s t_m + O(x^2) \quad (10)$$

A last configuration is K that is a fold-back version of J. The crosstalk performance of this concept can be expressed as

$$t_d x_s t_m + N \times t_d t_s x_m t_s t_m + x_d + O(x^2). \quad (11)$$

This configuration shows some improvement compared to the loop-back version J, but still the terms $t_d t_s x_m t_s t_m$ and x_d are present. Contrary to the improvement in crosstalk performance from configuration F to G, concept J is expected to have a degraded crosstalk performance since there is still a possibility for the light to directly access the wrong output.

D. Comparison of the Different Configurations

In order to make a good comparison of the performance of each of these architectures we have to look not only to the possible crosstalk paths but also to the losses.

1) Comparing the Number of Crosstalk Terms: In Table I, the first-order contributions in the desired output and those in the undesired output are listed for all eleven concepts. Configuration $A, E,$ and G all show the same number of first-order crosstalk contributions. Only the unavoidable term $t_d x_s t_m$ is present in the undesired output. This term is caused by the space switch and could only be avoided by preventing signals at the same wavelength to be routed through the same switch [15]. As mentioned before, this requires tunable (de)multiplexers and is too complicated for integration with the present state-of-the-art technology. This means that in first-order approximation no advantage is observed in using more than two PHASAR's. From the table it is also clear that the use of a single PHASAR always leads to a crosstalk penalty.

Configurations B and D, that use couplers instead of multiplexers, both exhibit up to $N-1$ additional first-order crosstalk terms. This is caused by the fact that no wavelength filtering is present after the switches. In concepts F and J, crosstalk from the demultiplexer directly accesses the outputs. These so-called loop-back configurations also show crosstalk terms originating from light that loops more than once though the switch. A disadvantage of loop-back configurations as has been addressed previously by Isida *et al.* [11], [12] is the coherent interference between crosstalk directly from the input in the output with the signal that passes the switch and the PHASAR and then reaches the output. In [12] concept K, which is a fold-back version of J, is proposed to avoid this coherent crosstalk. According to Table I there are still three first-order crosstalk terms present in the undesired output $(t_d x_s t_m, t_d t_s x_m t_s t_m,$ and $x_d)$. Because of the use of a hybrid arrangement in which the switches were simulated by changing fiber connectors, the switch crosstalk term x_s equaled $- \propto$ dB. Thus, only the last two terms were still present in the measurement results in [12], with x_d the dominant term. Since the length of the fibers used was also much longer than the coherence length of the light, coherent effects were hardly present. When integrating such structures, however, the path-lengths lie within the coherence length and signal-to-crosstalk beating will occur.

Architectures $C, H,$ and I show three first-order crosstalk terms. Besides the unavoidable term caused by the space switch, also a term originating from crosstalk generated at the demultiplexing operation and one from the multiplexing

TABLE I
FIRST ORDER CROSSTALK COMPONENTS IN THE 11 CONFIGURATIONS

Concept	Cross port (input 1- output 2)	Bar port (input 1- output 1)
A	$t_d x_s t_m$	$t_d t_s t_m$
B	$t_d x_s t_m$ + *(0 to N-1)* × $x_d t_s t_c$	$t_d t_s t_m$ + *(N-1 to 0)* × $x_d t_s t_c$
C	$t_d t_s x_m + t_d x_s t_m + x_d t_s t_m$	$t_d t_s t_m$
D	$t_d x_s t_m$ + *(N-1)* × $x_d t_s t_c$	$t_d t_s t_m$ + *(N-1)* × $x_d t_s t_c$
E	$t_d x_s t_m$	$t_d t_s t_m$
F	$t_d x_s t_m$	$t_d t_s t_m + x_d + t_d t_s x_m t_s t_m$
G	$t_d x_s t_m$	$t_d t_s t_m$
H	$t_d t_s x_m + t_d x_s t_m + x_d t_s t_m$	$t_d t_s t_m$
I	$t_d t_s x_m + t_d x_s t_m + x_d t_s t_m$	$t_d t_s t_m$
J	$x_d + t_d t_s x_m + t_d x_s t_m + x_d t_s t_m + t_d t_s x_m t_s t_m$	$x_d + t_d t_s t_m + t_d t_s x_m t_s t_m$
K	$t_d x_s t_m + N \times t_d t_s x_m t_s t_m + x_d$	$t_d t_s t_m$ + *(N-1 to 0)* × $t_d t_s t_m t_s x_m$

TABLE II
NUMBER OF FIRST- AND SECOND-ORDER CROSSTALK TERMS

Concept	Cross port (input 1- output 2)		Bar port (input 1- output 1)	
	O(x)	*O(x²)*	*O(x)*	*O(x²)*
A	*1*	*0 to N-1*	-	*N-1 to 0*
B	*1 to N*	*N-1 to 0*	*N-1 to 0*	*0 to N-1*
C	*3*	*2 × (N-1)*	-	*2 × (N-1) + 3*
D	*N-1*	*N*	*N-1*	*N*
E	*1*	*0 to 2 × (N-1)*	-	*(2× (N-1) to 0) + 1*
F	*1*	*1 to N*	*2*	*N-1 to 0*
G	*1*	*0 to N-1*	-	*N-1 to 0*
H	*3*	*4 × (N-1) + 2*	-	*4 × (N-1) + 5*
I	*3*	*4 × (N-1) + 2*	-	*4 × (N-1) + 5*
J	*5*	*6 × (N-1) + 3*	*2*	*6 × (N-1) + 6*
K	*N + 1*	*4 × (N-1) to 0 + 1*	*(N-1) to 0*	*5 × (N-1) to 0 + 3*

operation is present. These terms can occur since unidirectional traffic of multiple signals through a single PHASAR is possible.

In Table II, the number of second-order crosstalk terms is listed for all architectures. Again a large variety in numbers of crosstalk terms is visible. The *best* configurations show up to $N - 1$ second-order terms. Again these are unavoidable. In a worst case, the number of second-order crosstalk terms equals $6 \times (N-1) + 6$ (concept J). In practical applications, signals will be present at both inputs simultaneously. In a worst case approximation, these signals will be phase and polarization matched. The number of crosstalk terms present in that situation is found by adding the columns of the two ports in both tables.

2) Comparison of Signal Loss Properties: When comparing the different configurations in terms of losses a minimum number of PHASAR's is favorable for reasons of loss induced by a possible wavelength mismatch, as explained before. Also a simple layout is requested to minimize the number of waveguide crossings and keep the device as compact as possible, thus minimizing the propagation losses. Concepts A–D and J need 12 crossings, while the other concepts require 24 crossings. Typical losses at waveguide crossing are about 0.3 dB per crossing [7]. With nine crossings in a single path (worst case) this yields a loss penalty of 2.7 dB.

By crossing the slab regions of the PHASAR's used in the OXC the number of crossings can be drastically reduced [2]. To minimize wavelength mismatch between the PHASAR's, however, this position is not always favored. A gradient in the effective index over the wafer causes a linear shift in the central wavelength of the PHASAR. By positioning the PHASAR's in opposite orientation effects of a refractive index gradient over the wafer are opposite for both PHASAR's, which can cause large differences in central wavelength. In the case of positioning the PHASAR's above each other in the same orientation, both PHASAR's will experience a wavelength shift in the same direction as a result of such a gradient, and differences between the PHASAR's are minimized.

The use of 4×1 couplers as power-combiners inherently introduces an additional loss of -6 dB, and at the same time additional crosstalk components. The advantages are the wavelength *insensitive* response and the small size as compared to a PHASAR.

E. Conclusions

From the above analysis, it follows that in order to minimize the number of crosstalk terms one should avoid signals trav-

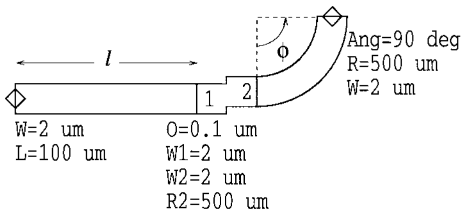

$$\begin{bmatrix} S_{11} & S_{12} \\ S_{21} & S_{22} \end{bmatrix} : \begin{bmatrix} 0 & e^{-j\beta_1 \ell} \\ e^{-j\beta_1 \ell} & 0 \end{bmatrix} \begin{bmatrix} 0 & \int U_1 U_2^* \\ \int U_1^* U_2 & 0 \end{bmatrix} \begin{bmatrix} 0 & e^{-j\beta_2^{\phi}\phi} \\ e^{-j\beta_2^{\phi}\phi} & 0 \end{bmatrix}$$

Fig. 3. S-matrix representation of a straight waveguide, a junction and a curved waveguide as used in the simulator.

eling unidirectional through a single PHASAR. This means that one should use at least two separate phased-arrays when constructing a 2 × 2 OXC. Configurations A, E, and G show the minimum amount of possible crosstalk terms. The crosstalk of the OXC is, in these cases, determined by the crosstalk of the switch and the square of the crosstalk of the PHASAR

$$x_{\text{oxc}}(:)xs + x_{d,m}^2.$$

Architecture A, however, needs four separate PHASAR's, instead of two as in E and G, and is thus unfavorable. To minimize the frequency mismatch of the PHASAR's they should be positioned as closely spaced as possible. In practice this means that configuration E is to be favored above G. In E, the PHASAR's can easily be positioned above each other, while in configuration G this would require many additional crossings, and thus additional losses.

III. Cross-Connect Simulations

From the previous section, it follows that configuration E is the most favored option for optimal crosstalk performance and configuration I (or H) the best option for avoiding frequency misalignment. Configuration I was the first one which we realized experimentally. Based on the present analysis we have also realized configuration E [8]. In the following, we will present the results of our simulation. The simulations were performed using an advanced CAD-tool for photonic integrated circuits that has been developed in our group [15] and is based on a professional microwave design system (HP's MDS). The simulation uses a scattering matrix description of the individual components (waveguides, couplers, PHASAR's) as in Fig. 3, and the full circuit's response follows from a matrix multiplication. The simulation accounts for transmission losses and radiation losses in waveguides, coupling losses at waveguide junctions and crossings, and includes effects of crosstalk contributions originating from the PHASAR and the switches. The simulator is capable of handling loops and bidirectional signal flows. For a more detailed description of the simulator, the reader is referred to [15].

Mach–Zehnder interferometer (MZI) switches used in integrated optical circuits typically show crosstalk values of −20 dB [20]. When used in a dilated scheme however, the crosstalk performance can be improved up to −40 dB [20]. In the simulations, we have considered both single-stage and double-stage switches and taken the crosstalk values −20 and −40 dB, respectively. The crosstalk performance of semiconductor

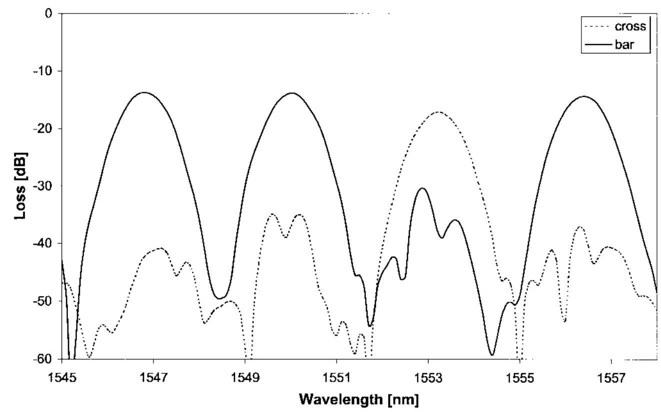

(a)

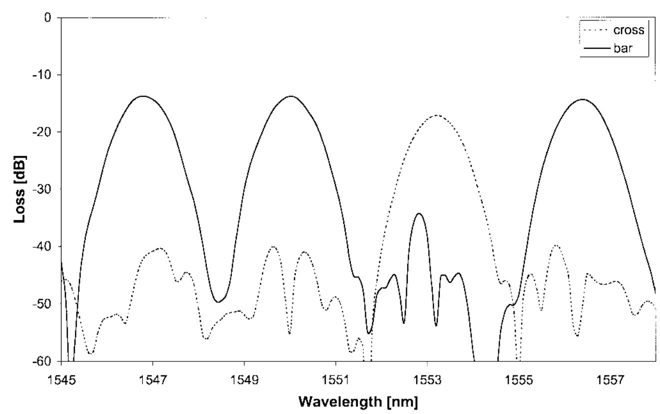

(b)

Fig. 4. (a) Simulated response of single PHASAR OXC using single-stage switches. (b) Simulated response of single PHASAR OXC using double-stage switches.

PHASAR demultiplexers is typically 20–25 dB [9]. When large PHASAR's are used, the −20 dB is more realistic; this is the value used in the simulation. The crosstalk value of the PHASAR in the simulation is set by adding a random phase-error to each of the array-arms sets. An average phase-error of 8° gives the crosstalk value of −20 dB.

In Fig. 4 the results of the simulations are depicted. The TE response is shown for the case of coupling light in input 1, and switching the second wavelength (The transverse magnetic (TM) response is comparable to that of TE. For reasons of clarity, we will restrict ourselves is the comparison to TE polarization). In situation (a) single-stage switches are used (−20 dB crosstalk), while in situation (b) the case with double-stage switches is simulated. The oscillating character of the crosstalk can be explained from the fact that the three main crosstalk contributions are all of the same order of magnitude. The terms $x_d t_s t_m, t_d t_s x_m$ and $t_d x_s t_m$ are all about 20 dB below the signal level. The oscillations in the response are caused by the path-length differences between the various crosstalk paths, due to the cumulation of three crosstalk contributions. Improving the switches does not improve the overall crosstalk performance of the OXC. The crosstalk term caused by the switches $(t_d x_s t_m)$ is reduced to −40 dB below signal level but still two terms of −20 dB remain that limit the overall OXC performance.

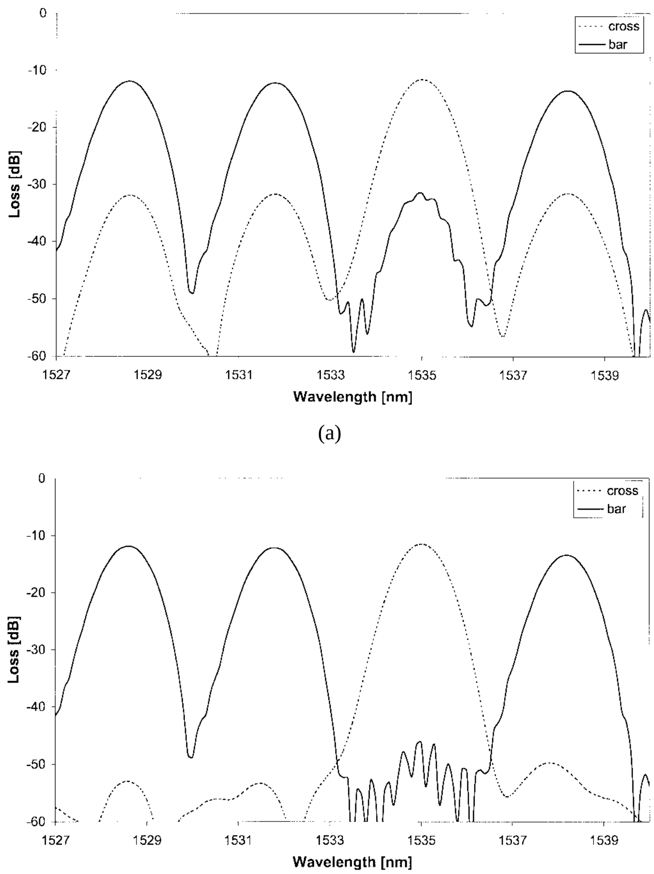

Fig. 5. (a) Simulated response of double PHASAR OXC using single-stage switches. (b) Simulated response of double PHASAR OXC using double-stage switches.

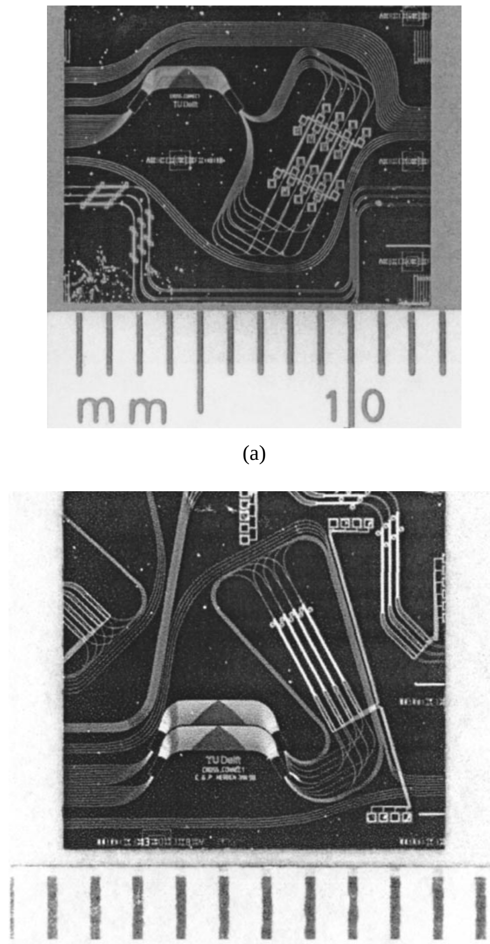

Fig. 6. Photographs of realized (a) single PHASAR OXC and (b) double PHASAR OXC.

In Fig. 5 the same situation is depicted for concept E. According to Table II the crosstalk is in first order only determined by the switch crosstalk $(t_d x_s t_m)$. Comparing Figs. 3(a) and 4(a) an improvement is visible in the response. The oscillating character of the crosstalk has disappeared except for the switched channel. The ripple in this channel is caused by interference between the $2(N-1)$ second-order crosstalk terms $(x_d t_s x_m)$. When the crosstalk of the switch is improved to -40 dB [Fig. 5(b)], the overall crosstalk of the OXC is also improved to about -40 dB. The oscillations in the second wavelength channel are still caused by the second-order crosstalk terms $x_d t_s x_m$, but this time also the first-order term $t_d x_s t_m$ is of the same order of magnitude and thus the ripple is more clear.

From the simulation results, we can conclude that the crosstalk of the configuration E OXC is determined by the switch crosstalk and the crosstalk of the individual PHASAR's is doubled

$$x_{\rm oxc}(:)x_s + x_{d,m}^2$$

Taking the experimental values as mentioned earlier, the effect of the PHASAR crosstalk will be negligible. In configuration I the crosstalk of the OXC is determined not only by the crosstalk of the switch but also by twice the crosstalk of the PHASAR

$$x_{\rm oxc}(:)x_s + 2x_{d,m}.$$

With the experimental values this gives three contributions of the same order of magnitude. Using dilated switches will reduce the effect of one of these three contributions, but the remaining two terms will still limit the overall crosstalk performance of this OXC configuration.

IV. Experimental Results

In this section, we compare the simulation results from the previous section with experimental results obtained from two integrated OXC configurations, which were recently realized in our group [7], [8]. The first consists of a single 16-channel polarization dispersion compensated PHASAR [17] and four electrooptical MZI space switches [19] connected in a fold-back configuration (configuration I). The second OXC using configuration E contains two eight-channel PHASAR's in stead of the single 16-channel PHASAR. Both OXC's are four-wavelength 2×2 OXC's using a channel spacing of 400 GHz (3.2 nm). Photographs of both devices are depicted in Fig. 6.

The PHASAR's have been made insensitive to the polarization by inserting a waveguide section with a birefringence different from the original waveguide structure in each array

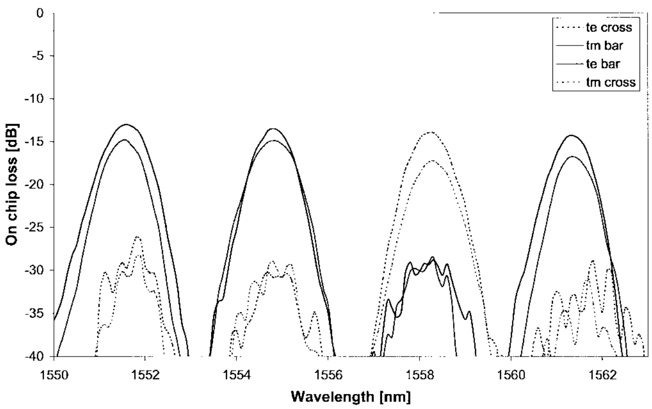

(a)

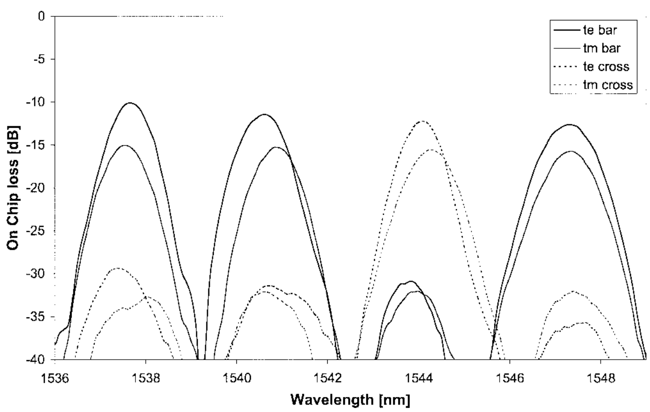

(b)

Fig. 7. Measures response of (a) single PHASAR OXC and (b) double PHASAR OXC, with the switch corresponding to the third wavelength channel switched on.

arm. The shape of this section is chosen such that the polarization dispersion of the total array is zero [17]. The 2×2 MZI switches have phase sections tilted 28° from the (011)-direction toward the (0-11)-direction to obtain polarization independent operation [19].

The OXC's were fabricated in a metal organic vapor phase epitaxy (MOVPE) grown InP/InGaAsP layer stack as described in [7], [8], and measured using the spontaneous emission spectrum of an erbium-doped fiber amplifier (EDFA) as a broadband light source and a polarizer to select the polarization. Light was coupled into the chip using microscope objectives, coupled out of the waveguides by a single-mode tapered fiber and analyzed using an optical spectrum analyzer.

In Fig. 7, the measured response is shown for both devices for TE polarization. (The response for TM-polarized light looks similar. For details see [7] and [8].) The transmission from input 1 to both output ports is depicted. In both cases the switch corresponding to the second wavelength channel is switched on, so that the second wavelength channel exits from output 2, while the other three wavelength channels exit from output 1. The on-chip losses of both devices are comparable (-13 dB for TE polarization). The crosstalk values, however, are quite different. The single-PHASAR OXC shows a crosstalk of -13 dB while in the case of the double-PHASAR OXC the crosstalk is -19 dB for TE polarization. For comparison: the performance of a single 2×2 MZI switch as used in both devices was measured to be -20 dB for TE polarization. This confirms the crosstalk performance as following from the simulations and analysis in the previous sections. In the double-PHASAR OXC the crosstalk of the OXC is determined by the crosstalk of the switch while in the single-PHASAR OXC the crosstalk is determined by interference between the crosstalk of the switch with twice the crosstalk of the PHASAR resulting in a crosstalk penalty in the order of 5 dB. The results for the single-PHASAR OXC [Fig. 7(a)] show a crosstalk of the total OXC, which is much poorer than the crosstalk obtained from the single switch. When we compare the response to the simulated one from the previous section [Fig. 5(a)] we can see a good agreement between simulation and measurement. The simulated value for the crosstalk agrees well and also the oscillating behavior is visible in both measurement and simulation. It is clear that the crosstalk performance of the whole OXC is worse than the single switch crosstalk.

In the double-PHASAR device the crosstalk values are in good agreement with those obtained from the single switch and a clear improvement compared to the single-PHASAR device is obtained. Experimental results are again in good agreement with the simulations.

V. Conclusions

A comparison has been made between different configurations of integrated optical OXC's. Eleven ways of constructing an N-wavelength 2×2 OXC have been compared semiqualitatively in terms of loss and crosstalk. Two configurations have been investigated in more detail, both numerical and experimental. For monolithic integration a minimum amount of separate PHASAR's is desired in order to avoid wavelength misalignment of the demultiplexers and multiplexers. In most configurations the OXC-crosstalk is determined by the sum of a number of switch and (de)multiplexer crosstalk terms. A comparison of coherent crosstalk contributions shows that for optimum performance multiple signals traveling unidirectional through a single PHASAR are unwanted. Optimum crosstalk performance can be obtained using a smart arrangement of two separate PHASAR's. In this arrangement, the (de)mux crosstalk is doubled and the switch crosstalk becomes dominant. With this arrangement OXC-crosstalk levels well below -30 dB are feasible with dilated switches and PHASARS with -20 dB crosstalk level. These conclusions are confirmed by extensive numerical simulations and experimental results.

References

[1] C. A. Brackett, A. S. Acampora, J. Sweitzer, G. Tangonan, M. T. Smith, W. Lennon, K.-C. Wang, and R. H. Hobbs, "A scalable multiwavelength multihop optical network: A proposal for research on all-optical networks," *J. Lightwave Technol.*, vol. 11, pp. 739–753, May/June 1993.

[2] K. Okamoto, M. Okuno, A. Himeno, and Y. Ohmori, "16-channel optical add/drop multiplexer consisting of arrayed waveguide gratings and double-gate switches," *Electron. Lett.*, vol. 32, no. 16, pp. 1471–1471, 1996.

[3] C. G. M. Vreeburg, T. Uitterdijk, Y. S. Oei, M. K. Smit, F. H. Groen, E. G. Metaal, P. Demeester, and H. J. Frankena, "First InP-based reconfigurable integrated add-drop multiplexer," *IEEE Photon. Technol. Lett.*, vol. 9, pp. 191–193, Feb. 1997.

[4] H. Li, C.-H. Lee, W. Lin, S. Didde, Y.-J. Chen, and D. Stone, "8-wavelength photonic integrated 2×2 WDM cross-connect switch using

$2 \times N$ phased-array waveguide grating (PAWG) multi-demultiplexers," *Electron. Lett.*, vol. 33, pp. 592–594, 1997.

[5] C. R. Doerr, C. H. Joyner, L. W. Stulz, and R. Monnard, "Wavelength-Division multiplexing cross-connect in InP" *IEEE Photon. Technol. Lett.*, vol. 10, pp. 117–119, Jan. 1998

[6] S. Suzuki, A. Himeno, and M. Ishii, "Integrated multichannel optical wavelength selective switches incorporating an arrayed-waveguide grating multiplexer and thermooptic switches," *J. Lightwave Technol.*, vol. 16, pp. 650–655, Apr. 1998

[7] C. G. P. Herben, C. G. M. Vreeburg, D. H. P. Maat, X. J. M. Leijtens, Y. S. Oei, F. H. Groen, J. W. Pedersen, P. Demeester, and M. K. Smit, "A compact integrated InP-based single-PHASAR optical cross-connect," *IEEE Photon. Technol. Lett.*, vol. 10, pp. 678–680, May 1998.

[8] C. G. P. Herben, D. H. P. Maat, X. J. M. Leijtens, Y. S. Oei, F. H. Groen, P. Demeester, and M. K. Smit, "Compact polarization independent optical cross-connect," in *Proc. 24th European Conf. Opt. Commun. (ECOC'98)*, Madrid, Spain, Sept. 20–24, 1998.

[9] M. K. Smit and C. van Dam, "PHASAR-based WDM-devices: Principles, design and applications," *IEEE J. Select. Topics Quantum Electron.*, vol. 2, pp. 236–250, June 1996.

[10] Y. Tachikawa, Y. Inoue, M. Kawachi, H. Takahashi, and K. Inoue "Arrayed-waveguide grating add-drop multiplexer with loop-back optical paths," *Electron. Lett.*, vol. 29, no. 24, pp. 213–2134, 1993.

[11] H. Takahashi, O. Ishida, K. Oda, and H. Toba, "Anticrosstalk arrayed-waveguide add-drop multiplexer with fold-back paths for penalty free transmission," *Electron. Lett.*, vol. 30, no. 24, pp. 2053–2055, Nov. 1994.

[12] O. Ishida, H. Takahashi, S. Suzuki, and Y. Inoue "Multichannel frequency-selective switch employing an arrayed-waveguide grating multiplexer with fold-back optical paths," *IEEE Photon. Technol. Lett.*, vol. 6, pp. 1219–1221, Oct. 1994.

[13] Y. Tachikawa, Y. Inoue, M. Ishii, and T. Nozawa, "Arrayed-waveguide grating multiplexer with loop-back paths and its applications," *J. Lightwave Technol.*, vol. 14, pp. 977–984, June 1996.

[14] J. Zhou, R. Cadeddu, E. Casaccia, C. Cavazzoni, and M. J. O'Mahony, "Crosstalk in multiwavelength optical cross-connect networks," *J. Lightwave Technol.*, vol. 14, pp. 1423–1435, June 1996.

[15] X. J. M. Leijtens, P. Le Lourec, and M. K. Smit, "S-matrix oriented CAD-tool for simulating complex integrated optical circuits," *IEEE J. Select Topics Quantum Electron.*, vol. 2, pp. 247–262, June 1996.

[16] M. Gustavsson, L. Gillner, and C. P. Larsen, "Statistical analysis of interferometric crosstalk: Theory and optical network examples," *J. Lightwave Technol.*, vol. 15, pp. 2006–2019, Nov. 1997.

[17] C. G. M. Vreeburg, C. G. P. Herben, X. J. M. Leijtens, M. K. Smit, F. H. Groen, J. J. G. M. van der Tol, and P. Demeester, "A low-loss 16-channel polarization dispersion compensated PHASAR demultiplexer," *IEEE Photon. Technol. Lett.*, vol. 10, pp. 382–384, Mar. 1998.

[18] P. Le Lourec, X. J. M. Leijtens, C. G. M. Vreeburg, T. Uitterdijk, C. G. P. Herben, and M. K. Smit, "S-matrix oriented simulation of a looped-back four channel add-drop multiplexer," in *Proc. 8th European Conf. Integrat. Opt. (ECIO '97)*, Stockholm, Sweden, 1997, pp. 18–21

[19] R. Krähenbühl, R. Kyburz, W. Vogt, M. Bachmann, T. Brenner, E. Gini, and H. Melchior, "Low-loss polarization insensitive InP/InGaAsP optical space switches for fiber optical communications," *IEEE Photon. Technol. Lett.*, vol. 8, pp. 632–634, May 1996.

[20] T. Uitterdijk, C. G. M. Vreeburg, D. H. P. Maat, F. H. Groen, H. van Brug, and I. Moerman, "Dilated, polarization insensitive InP-based space switch," in *Proc. 8th European Conf. Integr. Opt. (ECIO'97)*, Stockholm, Sweden, 1997, pp. 551–554.

[21] Y. S. Oei, L. H. Spiekman, F. H. Groen, I. Moerman, E. G. Metaal, and J. W. Pedersen, "Novel RIE-process for high quality InP-based waveguide structures," in *Proc. 7th European Conf. Integr. Opt. (ECIO'95)*, Delft, The Netherlands, 1995, pp. 205–208.

Chretien G. P. Herben was born in Sittard, The Netherlands, on October 10, 1972. He received the M.S. degree in applied physics from the University of Twente, Twente, The Netherlands, in 1996. His thesis was carried out in the Applied Optics Group and concerned the design and characterization of a scanning imaging confocal Raman microscope. In December 1996, he began pursuing the Ph.D. degree at Delft University of Technology in the Photonic Integrated Circuits Group of the Faculty of Information Technology and Systems, Delft, The Netherlands. The subject of his research was advanced integrated optical components for dense wavelength division multiplexed network applications with as main topic the design, fabrication, and characterization of integrated optical cross-connect chips.

Xaveer J. M. Leijtens was born in Uithoorn, The Netherlands, on April 6, 1962. He received the M.S. degree with honors in physics from the University of Amsterdam, Amsterdam, The Netherlands, in 1988. Subsequently, he started research work for the Dutch National Institute for Nuclear and High Energy Physics at CERN and received the Ph.D. degree in 1993.

He then joined the Photonic Integrated Circuits Group at the Delft University of Technology, Delft, The Netherlands. His current work is in the field of integrated optics and includes the design of multimode interference couplers, optical switches and PHASAR (de)multiplexers. He is working on the development of an advanced computer-aided design tool for photonic integrated circuits.

Peter Maat was born in Middelstum, The Netherlands, on November 8, 1969. He received the M.S. degree in applied physics from the University of Groningen, The Netherlands, in 1996. His thesis was carried out at the Research Group for Physics of Thin Films and Devices. There he studied losses in a Terahertz radiation detector (SIS-detector). In November 1996, he began pursuing the Ph.D. degree at Delft University of Technology, The Netherlands, at the Research Group for Optics.

He is currently concerned with the fabrication, characterization and improvement of electrooptical MZI-switches and more complex switch structures like dilated switches and switch-matrices.

Hans Blok (M'87) was born in Rotterdam, The Netherlands, on April 14, 1935. He received the degree in electrical engineering from the Polytechnical School of Rotterdam, The Netherlands, in 1956. He then received the B.Sc. and M.Sc. degrees in electrical engineering and the Ph.D. degree in technical sciences, all from the Delft University of Technology, Delft, The Netherlands, in 1961, 1963, and 1970, respectively.

Since 1968, he has been a Member of the Scientific Staff of the Laboratory of Electromagnetic Research at the Delft University of Technology. During these years, he carried out research and lectured in the areas of signal processing, wave propagation, and scattering problems. During the academic year 1970–1971, he was a Royal Research Fellow in the Department of Electronics of the University of Southamtpon, Southampton, U.K., where he was involved in experimental and theoretical research on lasers and nonlineair optics. In 1972, he was appointed Associate Professor at the Delft University of Technology, and in 1980 he was named Professor. From 1980 to 1982, he was Dean of Faculty of Electrical Engineering. During the academic year 1983–1984 he was Visiting Scientist at Schlumberger-Doll Research, Ridgefield, CT. At present, his main research interest is in inverse scattering problems and guided-wave optics.

Meint K. Smit (A'93) was born in Vlissingen, The Netherlands, in 1951. He receievd the M.S. and Ph.D. degrees (both with honors) in electrical engineering from the Delft University of Technology, Delft, The Netherlands, in 1969 and 1974, respectively.

In 1974, he was a Research Scientist with the NIWARS (Netherlands Interdepartmental Working Group on Application of Remote Sensing Technology). In 1976, he joined the Delft University of Technology as an Assistant Professor with the responsibility for research in microwave remote sensing and FM-CW radar development, and switched to optical communication in 1981, where he has set up facilities for fabrication of silicon-based integrated optical devices. He invented the phased array wavelength demultiplexer, which is presently being widely applied. He has been working on design of multimode interference couplers, optical switches, measurement and characterization of electrooptical devices and development of computer-aided design tools. From 1991 to 1992, he was on leave at the Institute of Quantum Electronics, ETH Zurich, Switzerland, where he worked on development of a fast and compact polarization independent optical switch.